Computers & Intelligent Decision Applications

Journal homepage: www.cidai-journal.org
eISSN: 3123-125X

Exchange Rate Volatility and Banking Sector Stability in Türkiye: Quantile Asymmetries, Time-Frequency Co-Movement and the Regulatory Ratio Illusion

Abdullah Kürşat Merter[1,*]

[1] Department of Business Administration, Faculty of Business Administration, Gebze Technical University, Kocaeli, Türkiye

ARTICLE INFO

Article history:
Received 14 May 2026
Received in revised form 17 June 2026
Accepted 5 August 2026
Available online 13 August 2026

Keywords:
Exchange rate volatility; Banking stability; Quantile-on-quantile regression; Wavelet coherence; Regulatory forbearance; Financial decision support.

ABSTRACT

Banking sectors in emerging economies remain exposed to currency shocks because foreign exchange liabilities sit on the balance sheets of both banks and their borrowers. The applied literature has largely treated this exposure as a single average effect, so an increase in volatility is assumed to act with the same sign and magnitude in tranquil and crisis months alike. That assumption merges the risk accumulating while the currency is calm with the mechanical distortion of reported ratios when it collapses, and it leaves open when, and at which cycle length, the relationship emerges. This study identifies the state-dependent structure of the link between exchange rate volatility and the stability of the Turkish banking sector and asks whether the observed patterns reflect underlying credit risk or the arithmetic of the ratios and the regulatory calendar. Monthly sector aggregates for non-performing loans, the capital adequacy ratio, and return on assets are examined against conditional volatility obtained from a generalised autoregressive conditional heteroskedasticity model with Student-t innovations. Wavelet coherence decomposes the relationship by calendar time and cycle length, quantile-on-quantile regression estimates the effect across pairs of quantiles in the two distributions, and quantile Granger tests establish the dominant direction. The estimates reveal a sign reversal. When the currency is calm, the effect on non-performing loans is positive and strengthens in the upper region of the credit risk distribution, whereas at the highest volatility states it turns negative. The capital ratio responds in opposite directions depending on where the sector stands, since severe shocks lift the reported ratio when capital is weakest and depress it when capital is strongest. Profitability deteriorates even in tranquil states, and its apparent predictive power for volatility can be traced to valuation gains and losses embedded in monthly earnings. A falling non-performing loan ratio and an improving capital ratio during currency stress therefore cannot be interpreted as evidence of resilience, since loan revaluation inflates both denominators while classification windows and valuation permissions defer loss recognition. Supervisory assessment requires organic measures that strip out revaluation and forbearance, together with preventive tools that bind in tranquil periods.

* *Corresponding author.*
E-mail address: *akmerter@gtu.edu.tr*

1. Introduction

Banking systems in emerging economies carry a structural exposure to currency movements. Currency crises travel across borders and bind national financial systems to a shared source of disturbance, as Eichengreen *et al.*, [1] first documented for industrial countries. Gaies *et al.*, [2] show that the stability of the exchange rate and the composition of external liabilities belong among the decisive determinants of banking crisis probability in developing economies, with debt liabilities raising crisis risk while foreign direct investment liabilities lower it. Two channels carry this exposure into bank balance sheets. The first is currency mismatch. When the domestic currency weakens, the local currency burden of foreign exchange obligations rises for banks and for their borrowers, and credit supply contracts. Akinci and Queralto [3] derive this amplification in a two-country model in which dollar debt and deviations from uncovered interest parity interact. Abbassi and Bräuning [4] identify it in supervisory loan-level data on net currency mismatches, and Kadırgan [5] traces the same balance sheet channel in the response of emerging market economies to capital flow shocks. The second channel is credit risk. Kuzucu and Kuzucu [6] find that depreciation is significantly associated with non-performing loans in emerging economies after the global financial crisis, although output growth remains the dominant macroeconomic determinant across country groups.

Regulation does not necessarily eliminate this exposure. Ahnert *et al.*, [7] show that macroprudential foreign exchange rules reduce bank foreign currency borrowing while firms respond by issuing more foreign currency debt directly, so vulnerability is displaced rather than removed. Fischer and Yeşin [8] report a related displacement in Central and Eastern Europe, where conversion programmes reduced Swiss franc mismatches at the cost of larger mismatches in other foreign currencies. External conditions add a further layer. Avdjiev *et al.*, [9] establish the dollar as a global risk factor whose appreciation depresses investment among dollar-indebted firms, while Bruno and Shin [10] and Borio and Zhu [11] articulate the risk-taking channel through which accommodative financial conditions raise leverage and loosen lending standards.

Türkiye lies at the intersection of these channels. Caglayan *et al.*, [12] document that deposit dollarization passes only partially into credit dollarization in Turkish banking, so that banks carrying wider mismatches extend more domestic credit and absorb more currency risk. Demirkılıç [13] shows for Turkish non-financial firms that foreign currency debt and mismatch depress capital investment following depreciation, which confirms that currency shocks reach the real sector through balance sheets before returning to banks as credit losses. Kasman *et al.*, [14] find exchange rate volatility to be a significant determinant of the stock returns and return volatility of Turkish banks. The sector thus offers an informative setting for tracing how currency shocks enter bank balance sheets.

The empirical treatment of this relationship nonetheless rests on a restrictive premise. Mean-based specifications describe the link between volatility and bank stability as a symmetric linear continuum, so a unit increase in volatility is assumed to act identically whatever the state of the market. Two consequences follow. Averaging merges the risk that builds during tranquil periods with the mechanical distortion of reported ratios during severe stress and conceals both within one coefficient. The time and frequency dimensions disappear as well, leaving unanswered the question of when and at which horizon the relationship takes shape. Evidence from the connectedness literature runs against this premise. Ando *et al.*, [15] show that dependence in the tails of financial networks departs substantially from average dependence, and Baumöhl *et al.*, [16] find that tail interconnectedness among global banks intensifies markedly during crisis episodes. Wang *et al.*, [17] and Yousaf *et al.*, [18] report that spillover strengthens under extreme market conditions. Sim and Zhou [19], who introduced the quantile-on-quantile estimator, show that the effect of a shock varies in sign and magnitude across the quantiles of both the shock and the outcome, and Umar *et al.*, [20] confirm this pattern in an application to geopolitical risk. The recurring lesson is that the sign and strength of such relationships depend on the period, the frequency band and the position in the distribution.

This study addresses that gap. It examines the effect of exchange rate volatility on the stability indicators of the Turkish banking sector using quantile-on-quantile regression, Morlet wavelet coherence and Granger causality tests at the quantile level. The two principal tools are instruments rather than contributions, and their role is to expose state-dependent asymmetry and time-varying co-movement that averaging suppresses. Using 283 monthly observations from December 2002 to June 2026, three sector-level indicators are examined, namely the non-performing loan ratio, the capital adequacy standard ratio and monthly return on assets. The explanatory variable is conditional exchange rate volatility estimated from a generalised autoregressive conditional heteroskedasticity model with Student innovations. The analysis yields three results. The decline in the non-performing loan ratio under severe currency volatility reflects denominator inflation and regulatory forbearance rather than any genuine improvement in credit quality. Extreme currency shocks raise the reported capital adequacy ratio when sector capital is at its weakest and erode it when capital is at its strongest, a divergence consistent with valuation and classification discretion. The apparent causality running from profitability to volatility follows from the mechanical presence of foreign exchange gains and losses within monthly earnings rather than from any structural forecasting content. The study therefore places the denominator effect, the regulatory calendar and the asymmetric survival mechanisms of a dollarized banking sector within a single empirical framework, and it speaks to the emerging market banking stability literature and to the design of macroprudential surveillance.

2. Theoretical Background

2.1 Risk Accumulation in Tranquil Periods and Mechanical Distortion in Crises

The link between exchange rate volatility and bank credit risk combines two opposing mechanisms that dominate in different states of the market. During tranquil periods, low volatility signals the construction of risk rather than its absence. Borio and Zhu [11] set out the risk-taking channel, in which accommodative financial conditions raise risk appetite and relax lending standards. Bruno and Shin [10] show that a weak dollar accompanies leverage expansion among global banks and accelerates cross-border credit. At the firm level, Bruno and Shin [21] find that interest differentials encourage foreign currency borrowing and carry trade positions. Hardy and Saffie [22] document that non-financial corporations borrow short-term in foreign currency and re-lend the proceeds as trade credit, taking on an intermediation role outside the regulated perimeter. Acharya and Vij [23] demonstrate that this behaviour responds to regulation, since the carry trade relationship breaks down once interest rate caps on foreign borrowing tighten, which indicates that unhedged exposure does not recede on its own. The consequences appear once the currency turns. Kalemli-Özcan *et al.*, [24] find that the leverage of firms holding unhedged foreign currency debt rises sharply through the net worth effect of depreciation. Niepmann and Schmidt-Eisenlohr [25] show that depreciation raises the default probability of foreign currency borrowers, so losses return to bank balance sheets.

A second mechanism dominates during crises and pushes reported indicators in the opposite direction. Severe depreciation revalues foreign currency and foreign currency indexed loans in local currency terms, and the total loan base expands. The non-performing loan ratio then falls even when the stock of problem loans is unchanged, because its denominator has grown. This arithmetic is consistent with the trajectory identified by Ari *et al.*, [26], who find that non-performing loans follow an inverse U-shaped path across 88 banking crises, rising around the onset of the crisis and peaking several years later. Abbassi and Bräuning [4] show that currency risk transmitted through net mismatches also reshapes the composition of credit during depreciation episodes, and Akinci and

Queralto [3] establish that under imperfect financial markets currency dynamics generate endogenous fragility where mismatches are present. Risk accumulation in tranquil states and mechanical ratio distortion in stressed states are therefore distinct processes that occupy different regions of the same distribution.

2.2 Regulatory Forbearance and the Measurement of Capital

The second strand concerns forbearance and the reliability of reported capital. Supervisors in emerging economies frequently relax accounting rules when the currency comes under pressure, for instance by fixing the exchange rate applied in risk-weighted asset calculations or by extending the window before a loan must be classified as non-performing. Such measures obscure organic erosion of capital. Acharya *et al.*, [27] document that fiscally constrained European governments substituted guarantees and forbearance for full recapitalisation, and that forbearance pushed undercapitalised banks toward zombie lending. Faria-e-Castro *et al.*, [28] show that concentrated lenders roll over troubled loans in order to raise the probability of repayment on existing exposures, and Tantri [29] identifies the same behaviour in loan-level data. Blattner *et al.*, [30] find that weak banks direct credit toward firms whose losses remain concealed, so that ratio-based capital regulation distorts the allocation of credit. Detection is difficult. Kashyap *et al.*, [31] show that indirect evergreening through related parties escapes regulatory audits, while Bonfim *et al.*, [32] find that on-site inspection reduces the probability of refinancing a zombie firm by about a fifth, which implies that reported loan quality reflects supervisory intensity as much as borrower condition. Chopra *et al.*, [33] report that an asset quality review in India doubled the declared delinquency rate, and that cleanups unaccompanied by recapitalisation deepened zombie lending. Álvarez *et al.*, [34] provide a taxonomy separating distressed firms, zombie firms and zombie lending, and Bassi *et al.*, [35] show that banks contract repo activity around reporting dates to present more favourable regulatory metrics.

Capital ratios are also managed through their denominators. Mariathasan and Merrouche [36] find that risk-weight density declines after internal model approval, most visibly at weakly capitalised banks. Behn *et al.*, [37] establish that model-based regulation leaves room for systematic underreporting of risk, and Plosser and Santos [38] show that banks under capital pressure report lower default probabilities for identical borrowers. Böhnke *et al.*, [39] find that the convergence of risk-weighted asset densities cannot be explained by bank size, losses, country risk or implementation timing, which points to arbitrage within the internal ratings-based approach, and Ferri and Pesic [40] reach a similar conclusion from the cross-sectional dispersion of those densities. Mayordomo *et al.*, [41] identify inflated housing appraisals as a channel that lowers risk weights, and Choi *et al.*, [42] show that leverage constraints induce banks to manage the risk composition of assets. Anginer *et al.*, [43] find that the effect of post-crisis capital regulation on bank risk is not uniform and depends on bank characteristics and the period examined. Taken together, this evidence implies that published capital and asset quality ratios need not reflect economic conditions during currency stress.

2.3 Rationale for the Empirical Design

The third strand concerns method. Mean regressions dissolve the configurations that characterise banks under extreme stress into a central effect. Shaddady and Moore [44] show that the influence of regulation and supervision on bank stability differs across the distribution of stability itself, so that a quantile design is required to recover it. Ando *et al.*, [15] treat tail spillover as the operative measure of systemic fragility, Baumöhl *et al.*, [16] show that tail interconnectedness intensifies during crises, and Wang *et al.*, [17] find that cross-market spillover strengthens under extreme conditions. Jang *et al.*, [45] argue that causality tests formulated in quantiles accommodate non-linear dependence that mean-based tests fail to detect. Sim and Zhou [19] provide the estimator that maps an effect across the distributions of both variables, and Qiao *et al.*, [46] demonstrate that wavelet coherence separates co-movement by calendar period and frequency horizon. This combination is required here for a specific purpose, namely to separate risk accumulation in tranquil states from mechanical distortion in stressed states.

3. Data and Methodology

This section describes the data set, the variable definitions and the sequence of econometric procedures. The analysis proceeds in four stages. Conditional USD/TRY volatility is first generated from a GARCH(1,1) model with Student innovations estimated on daily returns. Co-movement between volatility and the banking indicators is then examined in the time-frequency domain through Morlet wavelet coherence. In the third stage, the quantile-on-quantile estimator of Sim and Zhou [19] measures how the effect of volatility varies across the distributions of both variables.

3.1 Data and Variables

The study uses monthly data with 283 observations covering December 2002 to June 2026. In specifications that include control variables the sample is restricted to December 2003 through December 2025, giving 265 observations, because of the availability limit of the consumer price series.

Banking indicators are compiled as sector aggregates from the Turkish Banking Sector Monthly Bulletin of the Banking Regulation and Supervision Agency. Three dependent variables are used. NPL is the ratio of gross non-performing loans to total cash loans and captures realised credit risk. CAR is the capital adequacy standard ratio and reflects the capacity to absorb shocks. ROA is monthly return on assets in annualised percentage terms. Examining the three together allows the risk, capital and profitability dimensions of sector stability to be monitored within one framework.

The profitability ratios published in the bulletin are constructed by annualising cumulative within-year amounts, which imposes an artificial seasonality that resets each January. The profitability series used here are therefore derived from cumulative net profit rather than taken from the published ratios. Within-month net profit is measured as the difference between two consecutive cumulative profit figures within the same calendar year. Monthly return on assets and return on equity follow from the ratio of this amount to the average asset and equity stock of the month, multiplied by twelve. The conversion removes the mechanical January discontinuity and aligns the profitability series with the analysis frequency.

The explanatory variable FXVOL is the within-month average of conditional volatility estimated by a GARCH(1,1) model with Student innovations on daily USD/TRY logarithmic returns. The daily exchange rate is constructed from European Central Bank reference rates by dividing EUR/TRY by USD/EUR. Reliability was assessed against the Yahoo Finance USDTRY record. Across 2268 common trading days the correlation between the two series is 0.99998 and the mean absolute deviation is 0.46 percent, which confirms that the cross rate reproduces market quotations.

Descriptive statistics additionally report three complementary series. ROE is monthly return on equity, produced by the same conversion method. NIM is the net interest margin and allows the interest component of profitability to be followed. dFX is the monthly exchange rate change and shows at a descriptive level how the level of the currency relates to the volatility series. These series do not enter the estimated models but provide background for the interpretation of the findings.

Five control series are used. The consumer price index comes from the OECD SDMX DF_PRICES_ALL database on the 2015 base, and the adjusted industrial production index from the OECD SDMX DF_KEI database. The policy rate is taken at end-month values from the official interest rate tables of the Central Bank of the Republic of Türkiye, using the overnight borrowing rate before

May 2010 and the one-week repo rate thereafter, and it is consistent with the OECD IRSTCI record. Within-month averages of the VIX index and the ten-year United States Treasury yield, both from the FRED database, proxy global risk appetite and external financial conditions. Credit growth completes the control set. Descriptive statistics appear in Table 1.

Two considerations motivate the monthly frequency. Banking indicators are published monthly, so this is the frequency at which they are naturally observed. In addition, the transmission of currency volatility into balance sheet items proceeds at a pace that monthly data can track. Averaging daily conditional volatility within the month preserves the high-frequency information while matching the frequency of the balance sheet series.

3.2 Measuring Exchange Rate Volatility

Volatility clustering and fat tails in exchange rate returns rule out an assumption of constant conditional variance. Volatility is therefore modelled within the generalised autoregressive conditional heteroskedasticity framework of Bollerslev [47]. The daily logarithmic return is defined as r(t) = 100(ln P(t) − ln P(t−1)), and the mean and variance equations are given in Eq. (1) and Eq. (2).

$$r_t = \mu + \varepsilon_t, \qquad \varepsilon_t = \sigma_t z_t, \qquad z_t \sim t(\nu) \tag{1}$$

$$\sigma_t^2 = \omega + \alpha\varepsilon_{t-1}^2 + \beta\sigma_{t-1}^2 \tag{2}$$

Eq. (1) expresses the return as a constant mean plus an innovation scaled by conditional standard deviation. Allowing the innovations to follow a Student distribution with ν degrees of freedom prevents extreme returns from contaminating the α and β estimates and inflating measured persistence. Eq. (2) writes conditional variance as a linear combination of the previous squared shock and the previous conditional variance, subject to ω > 0, α ≥ 0 and β ≥ 0. Estimation is by maximum likelihood.

Because the banking data are monthly, the daily conditional volatility series is aggregated. FXVOL is the arithmetic mean of the conditional standard deviations for trading days falling within the calendar month. This measure summarises within-month intensification of volatility in a single figure and reflects bursts of conditional variance more faithfully than an end-of-month reading.

3.3 Wavelet Coherence Analysis

Treating the relationship between volatility and banking indicators as constant places calm and crisis periods, and short and long cycles, on an equal footing. To decompose the relationship along both dimensions, coherence analysis based on the continuous wavelet transform is used, following Torrence and Compo [48] and Grinsted *et al.*, [49]. The Morlet wavelet with central frequency ω_0 = 6, given in Eq. (3), is adopted because it balances resolution in time against resolution in frequency and allows the scale parameter to correspond approximately to the Fourier period.

$$\psi_0(\eta) = \pi^{-1/4}\, e^{i\omega_0\eta}\, e^{-\eta^2/2} \tag{3}$$

The continuous wavelet transform of the series x(t) is defined in Eq. (4), where s is the scale parameter and n the translation parameter.

$$W_x(n,s) = \sqrt{\frac{\delta t}{s}} \sum_k x_k\ \psi_0^*\left(\frac{(k-n)\,\delta t}{s}\right) \tag{4}$$

Here δt is the observation interval and the asterisk denotes complex conjugation. The cross wavelet spectrum of two series is the product of the transform of the first and the conjugate transform of the second, and the squared wavelet coherence coefficient in Eq. (5) is the ratio of the smoothed magnitude of the cross spectrum to the product of the smoothed auto spectra.

$$R^2(n,s) = \frac{\left|S\left(s^{-1}W_{xy}(n,s)\right)\right|^2}{S(s^{-1}|W_x(n,s)|^2)\, S\left(s^{-1}\left|W_y(n,s)\right|^2\right)} \tag{5}$$

The smoothing operator acts along the time and scale axes, a step required because coherence would otherwise equal unity at every point. The coefficient lies between zero and one and generalises the correlation coefficient to the time-frequency domain, with high values indicating strong co-movement at the corresponding period and scale.

Statistical significance is assessed against a 95 percent bound derived from 300 Monte Carlo replications of AR(1) surrogate series. The region outside the cone of influence, where edge effects operate, is excluded from interpretation. Phase differences are read from arrow orientation, with rightward arrows indicating in-phase movement, leftward arrows anti-phase movement and vertical arrows a lead of one series over the other. The time-frequency framework is appropriate because the relationship under study is not homogeneous across periods or horizons. Shifts in the monetary policy regime, revisions to capital rules and stress episodes can each alter the strength and the sign of the link, and the coherence map records such change without collapsing it into one coefficient.

Phase information indicates the direction of co-movement but does not establish causality. Direction is therefore determined primarily from the quantile Granger tests set out in subsection 3.5.

3.4 Quantile-on-Quantile Regression

Standard quantile regression allows the effect of the regressor to vary across the conditional distribution of the dependent variable while holding the position of the regressor in its own distribution fixed. The quantile-on-quantile approach of Sim and Zhou [19] relaxes that restriction and estimates, by local linear quantile regression, the marginal effect of the regressor at its θ quantile on the τ quantile of the dependent variable. The specification appears in Eq. (6), the objective function in Eq. (7) and the loss function of Koenker and Bassett [50] in Eq. (8).

$$y_t = \beta_0(\theta,\tau) + \beta_1(\theta,\tau)\left(x_t - \hat{Q}_x(\theta)\right) + u_t \tag{6}$$

$$\hat{\beta}_0(\theta,\tau), \hat{\beta}_1(\theta,\tau) = \underset{\beta_0,\beta_1}{\operatorname{argmin}} \sum_t \rho_\tau \left(y_t - \beta_0 - \beta_1\left(x_t - \hat{Q}_x(\theta)\right)\right) K\left(\frac{\hat{F}_x(x_t)-\theta}{h}\right) \tag{7}$$

$$\rho_\tau(u) = u\left(\tau - \mathrm{I}(u<0)\right) \tag{8}$$

In Eq. (8), the indicator function returns unity when its argument holds. The Gaussian kernel in Eq. (7) attaches greater weight to observations whose position in the empirical distribution function lies closer to θ, so that estimation at each pair of quantiles uses local information drawn from states of the regressor in the neighbourhood of θ. The estimated slope is the marginal effect of volatility, conditional on volatility being in state θ, on the τ quantile of the banking indicator.

The baseline bandwidth is $h = 0.05$, with robustness assessed at $h = 0.10$. Confidence intervals are 95 percent intervals from 200 bootstrap replications. Estimation proceeds on a grid of 19 quantiles for θ and τ between 0.05 and 0.95 in steps of 0.05. Surface estimates display the full response function, while curve sections trace the path of the effect across θ at selected values of τ.

Within this study the estimator serves to identify the state combinations in which the sign and magnitude of the volatility effect change. Low values of θ correspond to calm currency conditions and high values to stress. Movement along τ shows how the effect differs between benign and adverse states of the indicator. Reading the surface in two dimensions recovers the state-conditional asymmetry that mean-based estimators suppress.

3.5 Quantile Granger Causality

Direction is tested at the quantile level following Chuang *et al.*, [51], whose framework extends the classical Granger test beyond the conditional mean and asks whether causality differs across quantiles of the dependent variable. The specification estimated at quantile τ is given in Eq. (9).

$$y_t = \alpha(\tau) + \sum_{i=1}^{p} \phi_i(\tau)\, y_{t-i} + \sum_{j=1}^{p} \delta_j(\tau)\, x_{t-j} + u_t(\tau) \tag{9}$$

Causality from the regressor to the dependent variable at quantile τ is tested through the restriction that all lagged coefficients on the regressor equal zero, with the Wald statistic in Eq. (10).

$$W(\tau) = n\, \hat{\delta}(\tau)'\, \hat{\Omega}(\tau)^{-1}\, \hat{\delta}(\tau) \tag{10}$$

In Eq. (10), the vector collects the quantile estimates of the lagged coefficients and the matrix is its covariance estimate. Alongside the individual quantile tests, the sup-Wald statistic in Eq. (11) provides a joint test over the entire grid and equals the largest Wald value on that grid.

$$\sup W = \sup_{\tau \in T} W(\tau) \tag{11}$$

The quantile set contains 19 points between 0.05 and 0.95 in steps of 0.05. Lag length is selected by the Bayesian information criterion. Tests are conducted in both directions for each pair, from volatility to the indicator and from the indicator to volatility, so that a dominant direction can be identified without ruling out feedback. Because the quantile test can deliver different verdicts at individual quantiles, it captures cases in which causality operates with unequal force in the tails and at the centre. Each Wald statistic follows a chi-square distribution with degrees of freedom equal to the number of restrictions. Since that number equals the lag length chosen for the direction in question, the 5 percent critical value differs across directions, and each panel of Figure 5 therefore carries the critical line corresponding to its own lag length.

4. Results

4.1 Descriptive Statistics and Unit Root Tests

Table 1 reports descriptive statistics for the main series.

The non-performing loan ratio averages 4.054 percent, with a minimum of 1.492 and a maximum of 17.518. The range reflects the passage of the sector from a period of heavy credit risk at the start of the sample to a low-risk configuration later on. Skewness of 3.033 and kurtosis of 9.612 describe a distribution with a long right tail. The capital adequacy ratio averages 19.066 percent, comfortably above regulatory minima, but moves within a wide band between 14.644 and 32.669. Monthly return on assets averages 2.043 percent, and its minimum of −5.705 identifies months in which the sector recorded losses.

Exchange rate volatility averages 0.724 and peaks at 5.568. Skewness of 3.999 and kurtosis of 26.270 describe a series composed of brief, intense episodes separated by long tranquil stretches, and the Jarque-Bera statistic of 8891.777 rejects normality decisively. The maximum monthly exchange rate change of 31.769 percent records the sharpest single-month depreciation in the sample. A policy rate ranging from 4.500 to 50.000 confirms that the sample spans markedly different monetary regimes. Normality is rejected at the 5 percent level for every series. Skewed, fat-tailed distributions of this kind imply that mean-based estimators will fail to capture tail behaviour, which supports the quantile approach adopted here.

Table 2 shows that the highest pairwise correlation among the explanatory and control variables is 0.578. Variance inflation factors computed on the same regressor set range from 1.31 to 2.00, well below the conventional threshold of 10, so multicollinearity does not threaten the controlled specifications reported in the robustness subsection.

Table 1
Descriptive statistics of the main series

Variable	n	Mean	Std. Dev.	Min	P25	Median	P75	Max	Skewness	Kurtosis	JB	JB p
NPL	283	4.054	2.784	1.492	2.787	3.216	4.347	17.518	3.033	9.612	1523.241	0.000
CAR	283	19.066	3.844	14.644	16.695	17.927	19.454	32.669	1.795	2.648	234.614	0.000
ROA	282	2.043	1.081	−5.705	1.393	1.842	2.617	5.112	−0.763	8.797	936.627	0.000
ROE	282	18.342	10.311	−42.732	12.241	16.056	23.096	56.333	0.259	5.003	297.223	0.000
NIM	283	2.283	1.359	0.000	1.187	2.150	3.235	6.461	0.488	−0.298	12.265	0.002
FXVOL	283	0.724	0.563	0.058	0.451	0.648	0.877	5.568	3.999	26.270	8891.777	0.000
dFX	282	1.184	4.730	−9.630	−1.396	0.907	2.817	31.769	2.304	11.861	1902.337	0.000
INF	277	1.343	1.752	−1.443	0.412	0.949	1.805	13.576	3.085	14.247	2782.070	0.000
IPG	282	5.768	8.561	−29.904	2.049	6.391	9.963	65.188	0.712	9.979	1193.898	0.000
POLR	283	16.798	12.408	4.500	7.500	14.000	19.375	50.000	1.359	0.804	94.776	0.000
CRG	271	31.848	16.039	−6.136	19.904	29.908	41.369	72.278	0.329	−0.536	8.125	0.017
VIX	283	19.136	7.913	10.125	13.992	17.273	21.813	62.669	2.427	8.435	1116.777	0.000
US10Y	283	3.105	1.136	0.624	2.170	3.011	4.146	5.110	−0.179	−1.078	15.203	0.000

Note. NPL is the ratio of gross non-performing loans to total cash loans, CAR the capital adequacy standard ratio, ROA monthly return on assets, ROE monthly return on equity and NIM the net interest margin, all in percent. FXVOL is the within-month average of conditional USD/TRY volatility, dFX the monthly exchange rate change, INF monthly consumer price inflation, IPG annual industrial production growth, POLR the policy rate, CRG annual credit growth, VIX the volatility index and US10Y the United States ten-year Treasury yield. JB denotes the Jarque-Bera statistic.

Table 2
Pearson correlation matrix of explanatory and control variables

	FXVOL	INF	IPG	POLR	VIX	US10Y	CRG
FXVOL	1.000						
INF	0.336***	1.000					
IPG	0.004	−0.008	1.000				
POLR	−0.148**	0.311***	−0.146**	1.000			
VIX	0.246***	0.019	−0.357***	−0.097	1.000		
US10Y	−0.128**	0.057	0.015	0.494***	−0.175***	1.000	
CRG	−0.033	0.329***	0.181***	0.344***	−0.050	0.578***	1.000

Note. ***, ** and * denote significance at the 1, 5 and 10 percent levels of the pairwise correlations. Variance inflation factors computed on the same regressor set range between 1.31 and 2.00.

Table 3 reports unit root tests with a constant term. Read jointly, the integration properties of the series are mixed. For FXVOL the ADF statistic of −6.144, the PP statistic of −7.409 and the KPSS statistic of 0.284 all support stationarity. For NPL, ADF and PP reject the unit root while KPSS rejects stationarity. For CAR, ADF rejects the unit root, PP does not, and KPSS again rejects stationarity. The tests also disagree for inflation and the policy rate. For the United States ten-year yield, ADF and PP fail to reject the unit root while KPSS rejects stationarity, so all three tests point to non-stationarity.

Because the procedures of Dickey and Fuller [52], Phillips and Perron [53] and Kwiatkowski *et al.*, [54] are built on different null hypotheses, disagreement of this kind is expected in a long sample containing structural breaks. The test of Zivot and Andrews [55], which permits a single endogenous break in the intercept, locates break dates that coincide with the major stress episodes of the period. These are August 2018 for NPL, September to November 2021 for inflation and return on assets, and the first half of 2022 for volatility and the policy rate. Once the break is admitted, stationarity is supported for FXVOL, dFX, INF, ROA, POLR and VIX. This mixed picture undermines frameworks that require a cointegration assumption across levels and differences. The quantile and wavelet based approach adopted here is compatible with such a data structure because it imposes no strict requirement on integration order.

Table 3
Unit root tests with a constant term

Variable	ADF	ADF p	PP	PP p	KPSS	KPSS p	ZA	ZA p	Break date
NPL	−3.144	0.023	−7.049	0.000	1.075	0.010	−4.016	0.343	2018-08
CAR	−5.003	0.000	−1.798	0.382	1.236	0.010	−4.525	0.112	2017-01
ROA	−3.076	0.028	−14.119	0.000	0.356	0.096	−5.794	0.001	2021-11
NIM	−3.002	0.035	−7.701	0.000	0.493	0.043	−3.946	0.384	2010-06
FXVOL	−6.144	0.000	−7.409	0.000	0.284	0.100	−7.274	0.000	2022-03
dFX	−14.345	0.000	−14.391	0.000	1.283	0.010	−12.327	0.000	2022-07
INF	−2.059	0.261	−9.251	0.000	1.325	0.010	−6.894	0.000	2021-09
IPG	−3.903	0.002	−5.929	0.000	0.189	0.100	−4.420	0.145	2020-05
POLR	−2.944	0.040	−2.235	0.194	0.640	0.019	−5.923	0.001	2022-12
CRG	−1.801	0.380	−2.357	0.154	0.382	0.085	−3.976	0.367	2021-08
VIX	−4.523	0.000	−5.163	0.000	0.119	0.100	−5.109	0.020	2011-11
US10Y	−1.607	0.480	−1.673	0.445	0.726	0.011	−4.377	0.161	2021-12

Note. ADF, PP and KPSS are applied with a constant term. ZA denotes the Zivot and Andrews [55] test with a single endogenous structural break in the intercept, and break dates are estimated by the test.

4.2 Conditional Variance Properties of Exchange Rate Volatility

Table 4 reports the GARCH(1,1) model with Student innovations estimated on 6297 daily USD/TRY logarithmic returns.

Every parameter is significant at the 5 percent level. The mean return of 0.0428 is positive and significant on a daily basis, which reflects the average depreciation of the lira across the sample. The ARCH coefficient of 0.1387 and the GARCH coefficient of 0.8613 sum to unity, indicating the borderline persistence associated with integrated conditional variance, in which volatility shocks decay very slowly. When the memory of volatility shocks is this long, a single currency shock can remain in the conditional variance for months and reach bank balance sheets in stages rather than at once. The estimated degrees of freedom of 5.4275 confirm that the return distribution is considerably heavier tailed than the normal and that the Student specification is warranted.

The diagnostics indicate that the variance equation is adequate. The Ljung-Box statistic on squared standardised residuals is 0.73 at ten lags and 1.35 at twenty lags, and the ARCH-LM statistic at ten lags is 0.73, so no conditional heteroskedasticity remains. Residual autocorrelation in levels, with a Ljung-Box statistic of 61.05 at ten lags, follows from restricting the mean equation to a constant and does not compromise the volatility measure, because the input used in the subsequent analysis is the conditional variance rather than the mean equation residual.

Figure 1 presents the four principal series over time. Increases in FXVOL coincide with the episodes of financial stress and currency pressure within the sample, and the persistence of elevated levels after each burst is consistent with the near-unit persistence reported in Table 4. NPL declines over a long horizon from its high initial level, CAR fluctuates within a wide band, and ROA shows that negative readings are infrequent but deep, with profitability deteriorating sharply during stress.

Table 4
GARCH(1,1) estimation with Student innovations for daily USD/TRY logarithmic returns

Parameter	Estimate	Std. Error	t-statistic	p-value
Panel A. Mean equation				
μ	0.0428***	0.0040	10.71	0.000
Panel B. Variance equation				
ω	0.0003**	0.0001	1.99	0.046
α_1 (ARCH)	0.1387***	0.0114	12.21	0.000
β_1 (GARCH)	0.8613***	0.0124	69.27	0.000
ν (degrees of freedom)	5.4275***	0.3008	18.04	0.000
Panel C. Diagnostics				
Observations (N)	6297			
Log-likelihood	−5631.17			
AIC	11272.34			
BIC	11306.08			
Ljung-Box Q(10)	61.05***			
Ljung-Box Q(20)	89.83***			
Ljung-Box Q^2(10)	0.730			
Ljung-Box Q^2(20)	1.350			
ARCH-LM(10)	0.730			

Note. *** and ** denote significance at the 1 and 5 percent levels. Volatility persistence is $\alpha_1 + \beta_1 = 1.000$. Q and Q^2 are Ljung-Box statistics on standardised residuals and on squared standardised residuals. Insignificant Q^2 and ARCH-LM statistics indicate that the variance equation captures conditional heteroskedasticity fully, while the significant Q statistics on levels follow from the constant mean specification and do not affect the volatility measure.

4.3 Co-Movement in the Time-Frequency Domain

Figure 2 presents Morlet wavelet coherence in three panels, in which white contours mark the 95 percent significance bound, shading marks the region outside the cone of influence and arrows indicate the phase relationship.

Significant cells between NPL and FXVOL account for 4.6 percent of the total area, and co-movement concentrates at short and medium cycles. In the two to four month band the share of significant cells is 10.6 percent and extends across 2004 to 2026, while in the four to eight month band the share rises to 20.9 percent over 2006 to 2026. Period averages of coherence in the two to sixteen month band peak at 0.485 during 2016 to 2018, followed by 0.358 in 2010 to 2012, 0.303 in 2003 to 2006 and 0.271 in 2022 to 2026. The strength of co-movement in 2016 to 2018 corresponds to the years in which political uncertainty and currency pressure intensified.

The phase distribution reveals the sign structure of this co-movement. Among significant cells, 69.8 percent of arrows indicate anti-phase movement, 16.0 percent a lead of volatility, 9.2 percent a lead of non-performing loans and 5.0 percent in-phase movement. The dominance of anti-phase arrows shows that at short cycles volatility and non-performing loans predominantly move in opposite directions. The pattern appears counter-intuitive but follows from two mechanical sources that the quantile estimates in subsection 4.4 confirm. The first is denominator inflation. Sharp depreciation revalues foreign currency and foreign currency indexed loans in lira terms, the total cash loan stock expands nominally, and the denominator of the ratio grows faster than the numerator can. The second is the timing of forbearance. Turkish supervision has repeatedly extended the permitted delay before a loan must be transferred to non-performing status during stress episodes, and a wider classification window postpones the appearance of deteriorated loans in the ratio until after the stress has passed. A volatility burst and the reported ratio can therefore move in opposite directions at short horizons, with the balance sheet recognition of risk arriving considerably later.

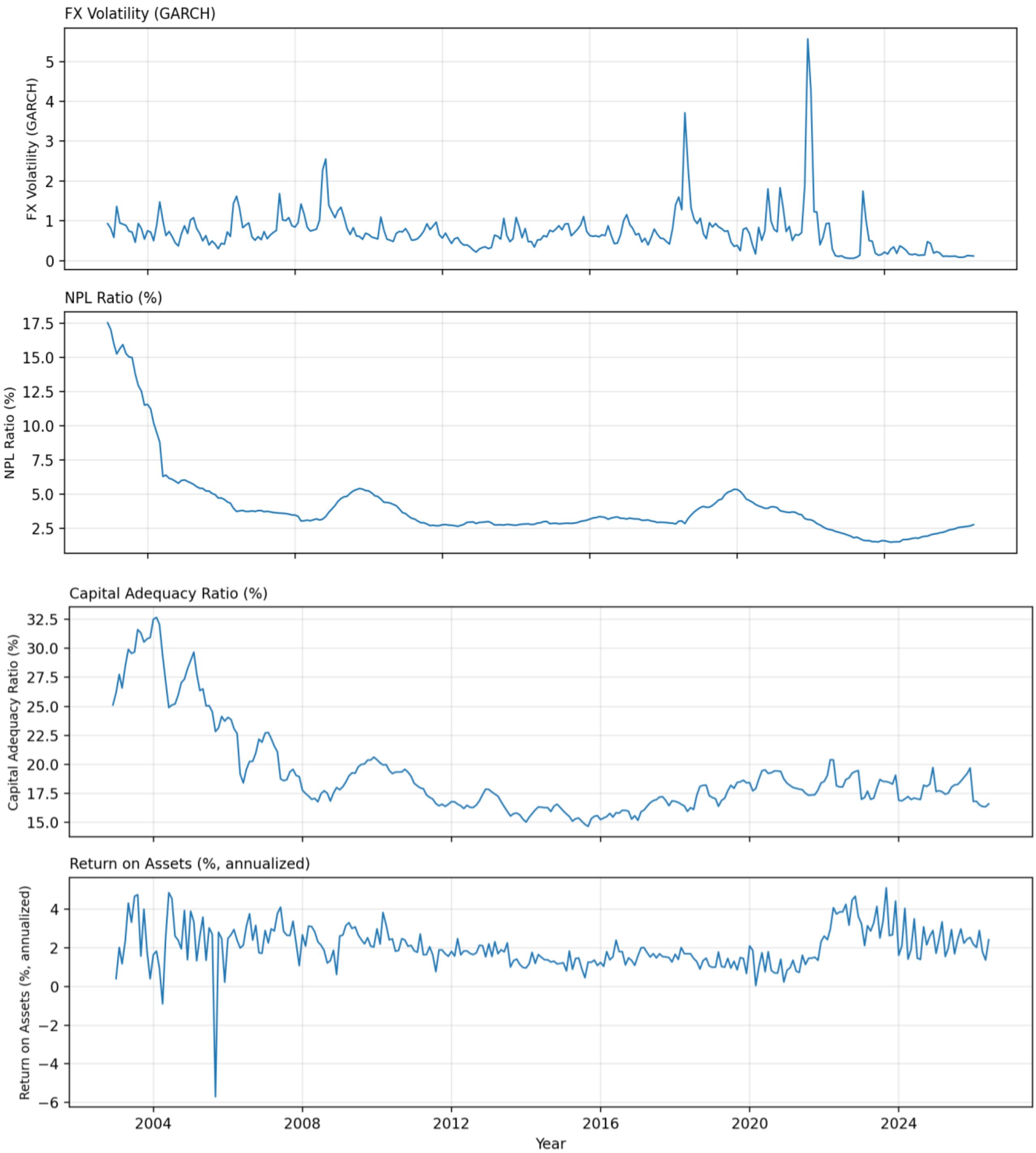

Fig. 1. Evolution of exchange rate volatility and the three banking stability indicators

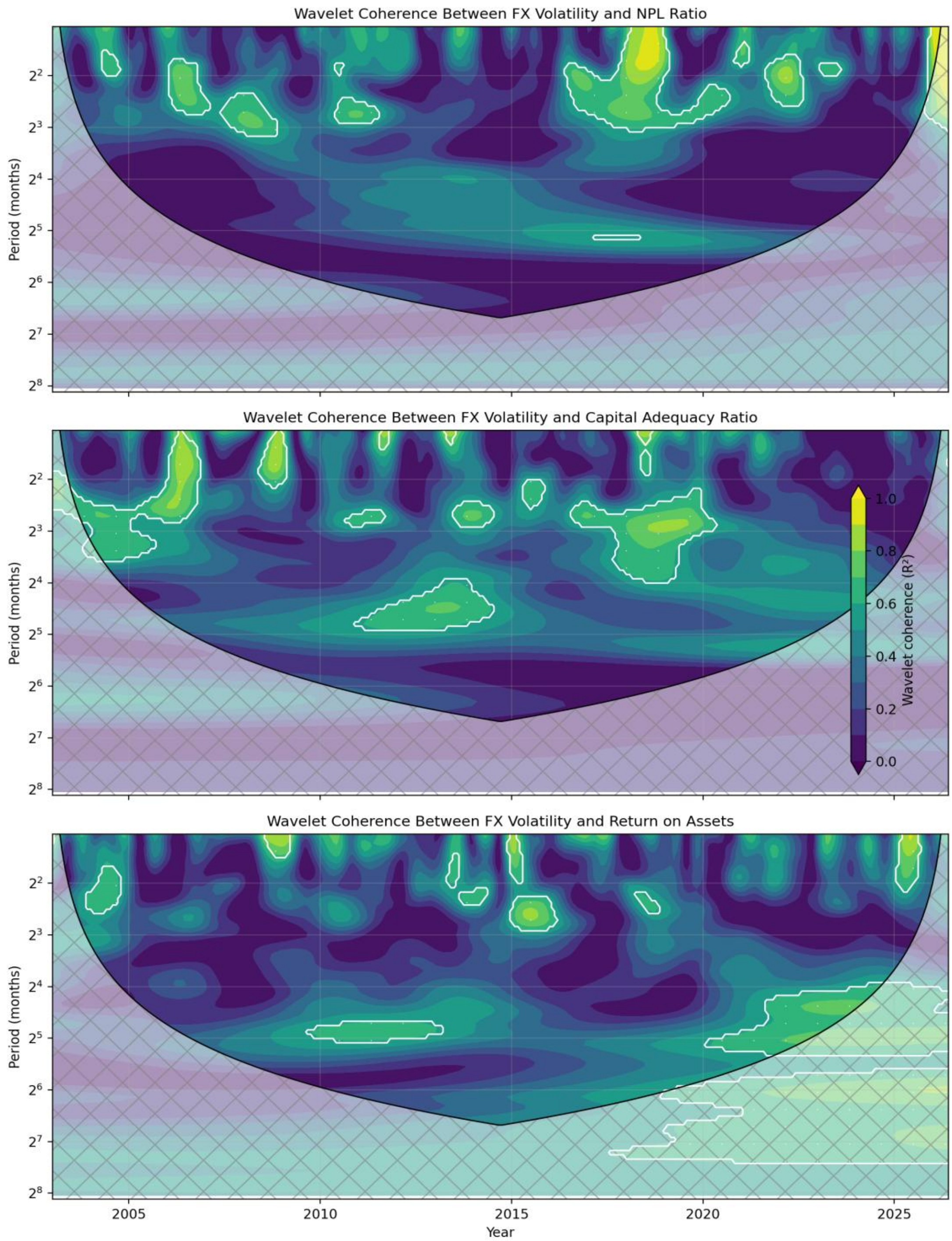

Fig. 2. Wavelet coherence between exchange rate volatility and the banking indicators. White contours denote the 95 percent significance bound, shading marks the region outside the cone of influence and arrows indicate the phase relationship

Significant cells between CAR and FXVOL account for 6.2 percent of the area, the highest share among the three indicators. Significance concentrates at 18.4 percent in the four to eight month band over 2003 to 2020 and at 10.3 percent in the eight to sixteen month band over 2004 to 2019. The remaining shares are 8.8 percent in the sixteen to thirty-two month band over the narrow 2010 to 2014 window and 6.3 percent in the two to four month band over 2006 to 2018. Period averages of coherence are 0.450 in 2003 to 2006, 0.416 in 2019 to 2021 and 0.408 in 2016 to 2018, and they fall to 0.191 in 2022 to 2026. The recent weakening suggests that capital ratio dynamics have become relatively detached from currency volatility, plausibly because of changes in the regulatory framework and of nominal balance sheet growth under high inflation.

The CAR phase distribution is more evenly divided, with 44.8 percent of arrows in anti-phase, 39.0 percent led by volatility, 10.8 percent led by the capital ratio and 5.5 percent in phase. A volatility lead in almost two fifths of significant cells indicates that currency movements precede adjustments in the capital ratio, which is consistent with the exchange rate elasticity of risk-weighted assets. Depreciation inflates the lira value of the foreign currency loan stock, risk-weighted assets expand and pressure accumulates on the ratio. Because that pressure materialises over the months following the shock rather than within it, the coherence map records a lead.

Significant cells between ROA and FXVOL account for 4.0 percent of the area, and here co-movement shifts toward long cycles. In the sixteen to thirty-two month band the share of significant cells is 13.2 percent over 2009 to 2024, against 6.4 percent in the four to eight month band over 2003 to 2025, 5.9 percent in the two to four month band and 3.0 percent in the thirty-two to sixty-four month band over 2010 to 2022. Period averages of coherence in the two to sixteen month band reach 0.355 in 2013 to 2015, 0.292 in 2022 to 2026 and 0.272 in 2019 to 2021. In the phase distribution a volatility lead dominates at 52.8 percent, with 21.8 percent anti-phase, 17.2 percent in phase and 8.2 percent led by profitability.

The concentration of co-movement at long cycles in the profitability panel carries an economic interpretation. Volatility reaches profitability through several channels operating at different speeds, namely valuation differences, realised foreign exchange results, provisioning expense and adjustments in the net interest margin. Because provisioning follows the realisation of credit risk and margin adjustment is slowed by maturity mismatch, the link between volatility and profitability becomes visible at the sixteen to thirty-two month scale. A volatility lead in more than half of the significant cells supports the reading that these channels activate sequentially after the shock rather than simultaneously with it.

4.4 Asymmetry of Quantile Effects

Quantile-on-quantile estimates show that the effect of volatility on the banking indicators depends both on the state of volatility itself and on the position of the indicator in its own distribution. Figure 3 presents the estimated surfaces, Figure 4 the coefficient curves at $\tau = 0.10$, 0.50, 0.75 and 0.90 with 95 percent bootstrap bands, and Table 5 the estimates at selected points with intervals from 500 bootstrap replications.

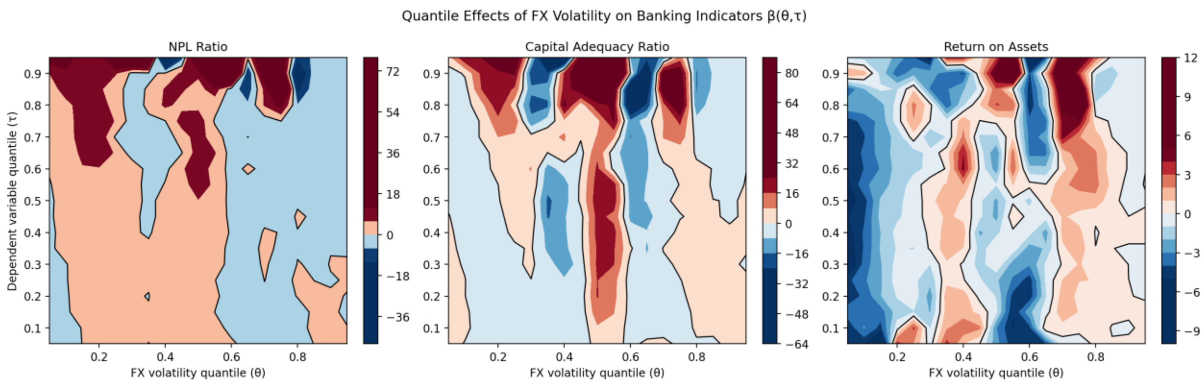

Fig. 3. Quantile-on-quantile surfaces of $\beta(\theta, \tau)$ for the three banking indicators

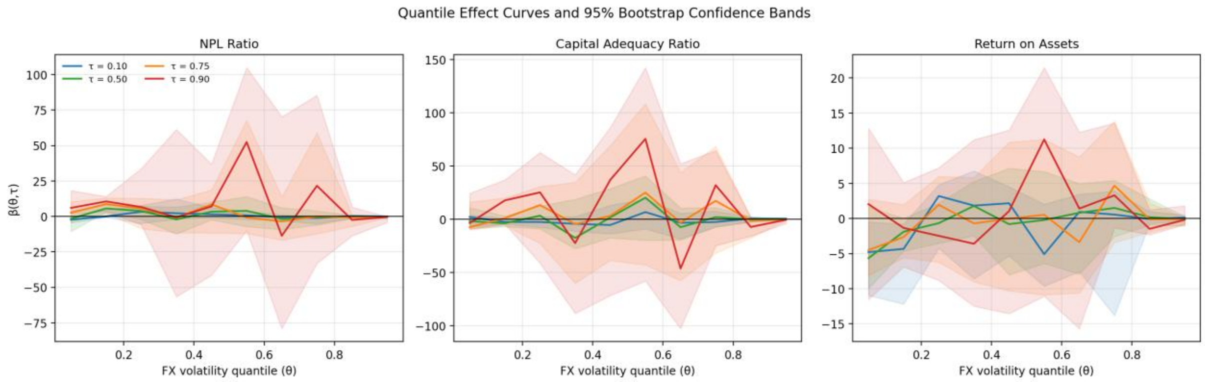

Fig. 4. Quantile-on-quantile β curves with 95 percent bootstrap bands at τ = 0.10, 0.50, 0.75 and 0.90

Table 5
Selected quantile-on-quantile estimates (h = 0.05)

Dependent variable	θ	τ	β(θ,τ)	95 percent bootstrap CI
NPL	0.10	0.50	4.017	[−2.873, 5.854]
NPL	0.10	0.75	3.450**	[1.463, 10.597]
NPL	0.10	0.90	10.579***	[1.907, 18.076]
NPL	0.50	0.50	5.784	[−2.007, 14.454]
NPL	0.90	0.50	−0.177	[−0.475, 0.190]
NPL	0.90	0.75	−0.325**	[−1.153, −0.149]
NPL	0.90	0.90	−0.572	[−2.700, 6.522]
CAR	0.90	0.10	0.618**	[0.106, 1.269]
CAR	0.90	0.90	−1.774	[−6.726, 4.853]
CAR	0.10	0.50	−4.286	[−7.891, 2.052]
ROA	0.10	0.10	−2.913**	[−10.560, −0.002]
ROA	0.10	0.50	−4.482***	[−6.401, −1.590]

Note. Confidence intervals are obtained from 500 bootstrap replications. ***, ** and * indicate that the 99, 95 and 90 percent bootstrap confidence intervals exclude zero.

Asymmetry in the NPL panel is pronounced. At low volatility, that is under calm currency conditions, the effect is strongly positive and grows in the upper region of the credit risk distribution. At θ = 0.10 the coefficient is 4.017 for τ = 0.50, 3.450 for τ = 0.75 and 10.579 for τ = 0.90. The two upper estimates are significant, and the increase from 3.450 to 10.579 as τ rises from 0.75 to 0.90 shows that risk accumulated during tranquil periods becomes visible primarily in states where the ratio is already elevated. The median estimate of 4.017 is positive but imprecise. At medium volatility the estimate at θ = 0.50 and τ = 0.50 is 5.784 and insignificant, since the interval contains zero. At high volatility the sign reverses. At θ = 0.90 the coefficients are −0.177, −0.325 and −0.572 for τ = 0.50, 0.75 and 0.90 respectively, with significance at τ = 0.75 and negative but imprecise estimates elsewhere.

Two period-specific mechanisms account for the reversal. Under calm currency conditions, low volatility encourages foreign currency and foreign currency indexed lending. When depreciation appears unlikely, banks extend such credit more readily and borrowers treat foreign currency liabilities as inexpensive. Risk accumulates without appearing on the balance sheet, and the transfer rate to non-performing status rises with a lag once the first depreciation wave arrives. The strengthening of the effect at the upper quantiles suggests that the episodes of most intense accumulation coincide with the fastest credit expansion. The negative coefficients at high volatility follow instead from two channels rooted in the construction of the ratio. Denominator inflation is the first. Sharp depreciation revalues the lira equivalent of foreign currency and foreign currency indexed loans, the total cash loan stock expands nominally, and the ratio falls because the numerator cannot grow at the same pace. Since the same revaluation enlarges risk-weighted assets, denominator inflation depresses both ratios at once. What differs between them is not the direction of movement but the informational content of that movement. A decline in the non-performing loan ratio conveys denominator growth rather than an improvement in credit quality, whereas a decline in the capital ratio conveys genuine deterioration, so the two indicators mirror each other in the signal they transmit. The second channel is the timing of forbearance. Repeated extensions of the permitted classification delay push the recognition of deteriorated loans beyond the stress window and bend the marginal relationship measured at high volatility toward the negative. The negative coefficients should accordingly be read as an artefact of ratio arithmetic and the regulatory calendar rather than as evidence of declining credit risk.

Asymmetry in the CAR panel runs in a different direction. At $\theta = 0.90$ the effect is significantly positive at 0.618 for $\tau = 0.10$, in the lower region of the capital distribution, and negative but imprecise at −1.774 for $\tau = 0.90$. At low volatility the estimate at $\theta = 0.10$ and $\tau = 0.50$ is −4.286 and insignificant. The exchange rate elasticity of risk-weighted assets explains the upper-quantile result. Where capital is already ample, a volatility shock pulls the ratio down, because depreciation inflates the lira equivalent of the foreign currency loan stock and expands risk-weighted assets while rising credit risk erodes earnings and hence the capital base through provisioning. The lower-quantile result requires a different account. Where capital is weak, the same shock supports the ratio, and this cannot be read as organic improvement. Two accounting channels operate together on the numerator and the denominator. On the numerator, the on-balance-sheet foreign currency position of the sector carries an asset surplus, so depreciation generates valuation and foreign exchange gains that pass through profit into equity. On the denominator, permission to value foreign currency items in the risk-weighted asset calculation at the lower exchange rates of earlier periods rather than at current rates defers the recognition of the shock in risk exposure amounts. Where capital is weak these channels reinforce one another and the measured coefficient turns positive, whereas where capital is strong, denominator inflation and provisioning pressure dominate and the coefficient remains negative. A single volatility shock can therefore produce oppositely signed effects depending on the position of the ratio in its distribution and on the regulatory provisions in force at the time.

In the ROA panel the effect is uniformly negative. Even at low volatility the coefficient at $\theta = 0.10$ and $\tau = 0.10$ is significantly negative at −2.913, and the estimate at $\theta = 0.10$ and $\tau = 0.50$ is −4.482 and significant at the 1 percent level. That volatility erodes profitability even during tranquil periods points to the continuity of the cost and provisioning channel. Currency fluctuations affect funding costs, the reserve requirement burden and valuation uncertainty in every state of the market, and that burden weighs most heavily where profitability is already thin. Significance at the lower quantile indicates that volatility operates as an additional source of pressure precisely when earnings capacity is weakest.

The surfaces in Figure 3 confirm that these point estimates describe the broader pattern. On the NPL surface the positive region concentrates in the corner combining low θ with high τ, while the negative region extends along the high θ axis. The curves in Figure 4 show that the effect changes sign smoothly across θ, so the finding does not rest on isolated grid points. The widening of the bootstrap bands at the tails records greater estimation uncertainty there, yet the sign structure is preserved within those bounds.

4.5 Quantile Causality Findings

Table 6 summarises the quantile Granger tests following Chuang *et al.*, [51], with lag lengths chosen by the Bayesian information criterion. Figure 5 shows the Wald profile by quantile for each of the six directions together with the corresponding 5 percent critical line.

Table 6
Quantile Granger causality summary

Direction	Lag	Significant quantiles (out of 19)	sup-Wald	5 percent critical value
FXVOL → NPL	6	14	22.07***	12.59
NPL → FXVOL	1	3	14.35***	3.84
FXVOL → CAR	1	9	16.61***	3.84
CAR → FXVOL	1	1	4.81**	3.84
FXVOL → ROA	3	2	4.10	7.81
ROA → FXVOL	1	11	8.04***	3.84

Note. Tests follow Chuang *et al.*, [51] and optimal lag lengths are selected by the Bayesian information criterion. The null hypothesis is the absence of Granger causality in the indicated direction. ***, ** and * denote rejection at the 1, 5 and 10 percent levels against chi-square critical values with p degrees of freedom.

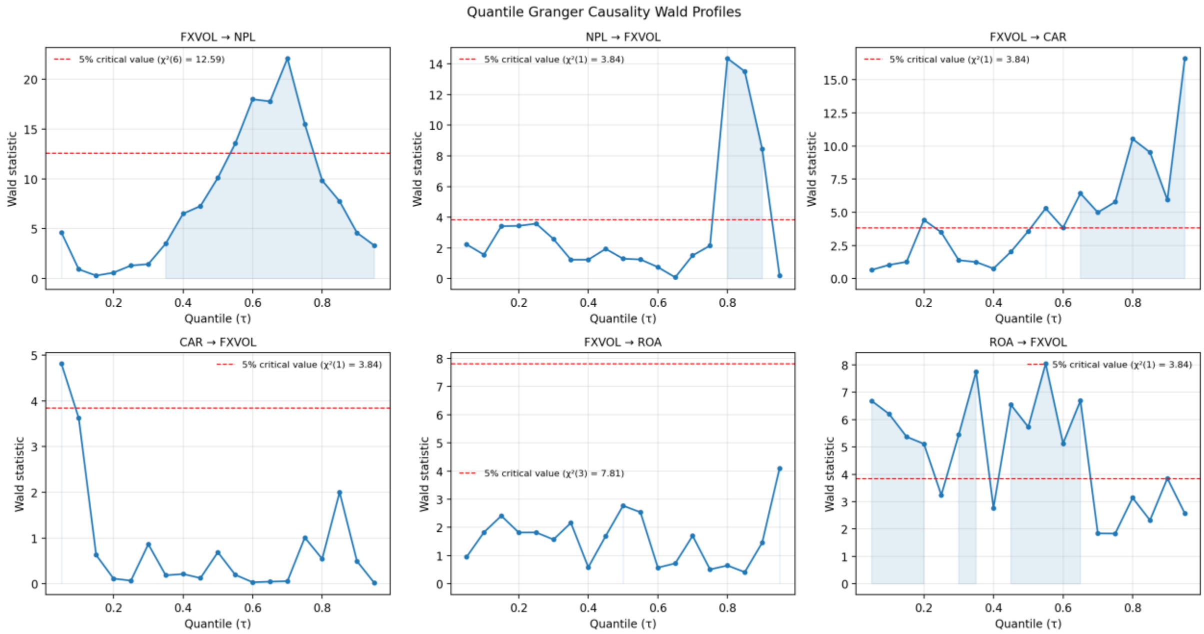

Fig. 5. Wald profiles by quantile for the six causality directions. Dashed lines denote the 5 percent chi-square critical value corresponding to the lag length of each direction

From FXVOL to NPL the null of no causality is rejected at 14 of the 19 quantiles, with a sup-Wald statistic of 22.07. Significance concentrates in the middle and upper quantiles, which indicates that volatility carries predictive content for credit risk mainly when non-performing loans stand at medium or high levels. The selected lag of six months is consistent with the accumulation mechanism, since the translation of a volatility signal into transfers to non-performing status extends over several quarters. In the reverse direction, causality from NPL to FXVOL is significant at only 3 quantiles with a weaker sup-Wald statistic of 14.35.

From FXVOL to CAR there is significance at 9 of the 19 quantiles with a sup-Wald statistic of 16.61, concentrated in the middle of the distribution. Predictive content for the capital ratio in this region suggests that risk-weighted asset adjustment and provisioning operate most actively at intermediate capital levels, where the ratio is neither cushioned by ample buffers nor supported by the accounting channels that dominate at the lower tail. The reverse direction from CAR to FXVOL is significant at a single quantile with a sup-Wald statistic of 4.81.

For ROA the configuration differs. From FXVOL to ROA significance appears at only 2 quantiles, whereas from ROA to FXVOL it appears at 11 with a sup-Wald statistic of 8.04. This asymmetry does not support a structural predictive interpretation. No economic channel allows aggregate bank profitability to forecast currency market volatility, so the result is better understood as the statistical signature of simultaneity. Foreign exchange results are a component of profitability, and currency movements and earnings therefore draw on the same monthly information set. When series are aggregated to monthly frequency, that shared component can generate an apparent cross-prediction. The finding also flags a potential endogeneity concern for the quantile-on-quantile estimates, which subsection 4.7 addresses. Given the strength and one-sidedness of the results for NPL and CAR, the conclusion that the dominant direction runs from volatility to the sector is retained.

Wavelet phase arrows are not treated as independent evidence on direction. The lead signals from the phase statistics are assessed jointly with the quantile Granger results. For NPL and CAR both approaches support a lead of volatility. For ROA they diverge, with the coherence map emphasising a volatility lead and the causality tests emphasising feedback from profitability. The divergence indicates that the profitability channel operates in both directions and that the two directions separate by frequency and forecast horizon.

4.6 Robustness Checks

Robustness is examined from three directions. The first concerns bandwidth. Repeating the baseline estimation with $h = 0.10$ preserves the sign pattern. Under the wider bandwidth the NPL coefficient is 3.499 at $\theta = 0.10$ and $\tau = 0.50$, 10.142 at $\theta = 0.10$ and $\tau = 0.90$, −0.155 at $\theta = 0.90$ and $\tau = 0.50$ and −0.689 at $\theta = 0.90$ and $\tau = 0.90$. For CAR the coefficient at $\theta = 0.90$ and $\tau = 0.90$ is −1.948, and for ROA it is −3.005 at $\theta = 0.10$ and $\tau = 0.10$ and −2.818 at $\theta = 0.10$ and $\tau = 0.50$. The signs of the significant points and the ordering of magnitudes survive, so neither the growth of the tranquil-period positive effect at the upper quantiles nor the crisis-period reversal is an artefact of kernel weighting.

The second concerns macroeconomic controls. Monthly inflation, annual industrial production growth, the policy rate, the VIX, the United States ten-year yield and credit growth are added to the specification, and partial quantile-on-quantile surfaces are re-estimated for December 2003 to December 2025 with 265 observations. The controlled surfaces reproduce the sign pattern of the baseline, and the full set of estimates appears in Table A1. Controlled coefficient ranges are −6.77 to 9.33 for NPL, −21.48 to 22.65 for CAR and −8.15 to 20.06 for ROA. For NPL and CAR the magnitudes contract substantially relative to the uncontrolled ranges of −42.33 to 77.18 and −57.12 to 86.26, which reflects both the absorption of variance by the controls and the reduction of omitted variable bias. For ROA the range is largely unchanged. Preservation of the sign structure indicates that the asymmetric response of the banking indicators to volatility is not an indirect reflection of inflation, real activity, monetary policy or global financial conditions.

The third concerns the measurement of volatility. Replacing the GARCH-based measure with realised volatility, computed as the square root of the sum of squared daily returns within the month, leaves the sign pattern intact. For NPL at $\theta = 0.10$ the coefficients are 0.980 at $\tau = 0.50$, 1.045 at $\tau = 0.75$ and 2.313 at $\tau = 0.90$, the last with a bootstrap interval of 0.548 to 2.996 and significantly positive. At $\theta = 0.90$ the coefficients are negative at all three values of τ. For ROA the coefficients at $\theta = 0.10$ with $\tau = 0.10$ and $\tau = 0.50$ are −1.020 and −0.832, significantly negative with intervals of −3.533 to −0.140 and −1.677 to −0.422. For CAR the coefficient at $\theta = 0.90$ and $\tau = 0.90$ retains its sign at −0.289. The causality results are similar, with significance at 14 quantiles from realised volatility to

NPL and at 5 to CAR, weak reverse directions, and feedback from profitability significant at 14 quantiles. Agreement between the two measures indicates that the results do not depend on a particular model of conditional variance. The GARCH measure is retained in the baseline because conditional variance describes within-period volatility dynamics in smoothed form and its monthly average aligns more closely with the frequency of the balance sheet data.

Considered together, the robustness exercises leave the central result intact. The relationship between exchange rate volatility and the stability indicators of the Turkish banking sector is asymmetric, varies across time and frequency, and runs predominantly from volatility to the sector. Risk accumulates through the credit channel during tranquil periods, while denominator inflation and the timing of forbearance govern the response during crises. The capital ratio responds through the exchange rate elasticity of risk-weighted assets and the valuation discretion applied to them, and profitability through the cost and provisioning channel. None of these mechanisms is sensitive to the bandwidth, the macroeconomic controls or the volatility measure.

4.7 Limitations

Three limitations qualify the findings. First, quantile-on-quantile regression measures conditional dependence and does not identify structural causality. The feedback detected from profitability to volatility exposes the simultaneity that arises when both variables draw on the same monthly information set, and the mechanical share of foreign exchange results within earnings prevents a full separation of the two directions. Second, the non-performing loan ratio is itself shaped by the regulatory calendar. Discretion over classification periods and over the exchange rates applied in risk-weighted asset calculations makes it difficult to separate the behaviour of reported ratios during stress from organic risk dynamics. This study treats that separation qualitatively and does not quantify it, which would require supervisory data on the loans held within extended classification windows and on the exchange rates applied in capital calculations. Third, the specifications with control variables end in December 2025 because of the availability limit of the consumer price series, so the extension of the baseline results into the first half of 2026 rests on the bivariate design. These limitations do not alter the direction of the central result, but they caution against reading the estimated magnitudes as structural parameters.

5. Discussion

5.1 Risk Accumulation in Tranquil Periods and the Mechanical Ratio Illusion

The first group of findings concerns credit risk. At the highest volatility quantile the effect on the non-performing loan ratio is negative across the upper half of the credit risk distribution, whereas at the lowest volatility quantile it is positive and grows sharply toward the upper tail. Quantile causality from volatility to non-performing loans holds at 14 of the 19 quantiles, coherence peaks during the 2016 to 2018 episode, and close to seven tenths of significant phase arrows indicate anti-phase movement. The configuration is internally consistent. Volatility carries predictive content for credit risk, yet the contemporaneous association reverses sign precisely where stress is most severe.

The negative sign at the stress quantiles cannot be read as an improvement in credit quality. Two artificial mechanisms generate it. Denominator inflation is the first. Severe depreciation raises the lira value of foreign currency loans and expands the total loan base, so the ratio declines even when the stock of problem loans is unchanged. The second is forbearance. Turkish supervisory practice has repeatedly extended the legal classification window during recent stress episodes and deferred loss recognition. Both mechanisms are consistent with the crisis database evidence of Ari *et al.*, [26], in which non-performing loans follow an inverse U-shaped path and peak well after the onset of the crisis rather than during it. Panel evidence that depreciation raises non-performing loans in emerging economies establishes the long-run direction [6], so the short-run negative sign belongs to ratio accounting rather than to credit fundamentals. Niepmann and Schmidt-Eisenlohr [25] provide the microeconomic counterpart, showing that the default risk of foreign currency borrowers materialises during depreciation episodes while reaching reported ratios only with a lag.

The mechanics of deferral are documented at the level of individual loans. Weak banks lend to firms whose losses remain concealed, which distorts the allocation of credit under ratio-based regulation [30]. Problem loans are refinanced so that recognition of the loss is postponed [28, 29], and evergreening routed through related parties escapes supervisory audit [31]. Undercapitalised banks turn to zombie lending where guarantees and forbearance substitute for recapitalisation [27], reported metrics are improved around reporting dates [35], and the cross-sectional dispersion of risk weights reflects comparable management on the capital side [40]. Bonfim *et al.*, [32] show that on-site inspection substantially reduces the refinancing of zombie firms, which implies that the observed ratio depends on supervisory intensity as much as on borrower condition. The anti-phase arrows and the negative stress-quantile coefficients are the aggregate expression of these microeconomic practices in Turkish banking. Read in isolation, the two would suggest that currency stress leaves credit quality intact. Read alongside the large positive coefficients at the tranquil-period quantiles, they describe a sequence in which exposure is built while the currency is calm and its recognition is deferred once the currency breaks. The finding that positive coefficients strengthen toward the upper tail of the ratio locates the accumulation, since the phases of most rapid foreign currency credit expansion are those whose consequences surface where the ratio is already elevated.

5.2 The Role of Regulatory Discretion in Capital Adequacy

The second group of findings concerns capital. Extreme currency shocks raise the reported capital adequacy ratio at the lowest capital quantile and depress it at the highest. A shock therefore improves the published ratio when sector capital is at its weakest and erodes it when capital is at its strongest, which inverts the ordering that a solvency measure should display.

Regulatory accounting discretion accounts for much of this inversion. When sector capital has been weak, Turkish supervisory practice has permitted risk-weighted assets to be computed at historical exchange rates, insulating the denominator, while realised currency gains have been allowed to flow through profit into equity, raising the numerator. The resulting buffer is not economic. Organic capital erodes under credit losses and maturity mismatch while the reported ratio conceals that erosion. When capital is strong the discretion is either unavailable or immaterial in size, and the shock registers as the burden it is. The cross-quantile sign reversal is consistent with the hypothesis that discretion becomes operative when the sector is weakest, which is also when its use is most tempting and least costly to authorise. The hypothesis cannot be tested directly on aggregate data, since the quantiles of a sector ratio order states of the sector over time rather than partition banks into weak and strong groups. Bank-level evidence establishes the mechanism, while the aggregate estimates locate its footprint in the time series.

The divergence aligns with the risk-weight management literature. Weakly capitalised banks lower risk weights through internal models as a matter of strategy [36], the discretion embedded in model-based regulation translates into systematic underreporting [37], and banks under capital pressure produce lower risk estimates for identical borrowers [38]. Convergence in risk-weight densities that true risk cannot explain confirms that arbitrage space exists within the internal ratings-based approach [39]. Inflated appraisals and the management of asset composition under leverage constraints extend the same behaviour to the accounting layer [41, 42], and post-crisis evidence indicates that the effect of capital regulation on bank risk depends on bank characteristics and on the period [43]. Martynova *et al.*, [56] show why the practice persists, since a supervisor unable to commit finds forbearance optimal after the fact even though it weakens incentives beforehand, which is the time inconsistency that valuation and classification permissions embody. Chopra *et al.*, [33,57] add the cost of delay, since cleanups unaccompanied by recapitalisation deepen zombie lending, so an artificial buffer defers the problem at the price of enlarging it.

5.3 Endogeneity and Implications for Macroprudential Policy

The third group of findings concerns direction and supplies the econometric counterpart of these distortions. Quantile causality from return on assets to volatility holds at 11 of the 19 quantiles, while the reverse direction holds at only 2. Taken at face value, profitability would appear to forecast currency volatility. The design does not support that reading. Foreign exchange gains and losses enter monthly profitability mechanically, so the sector books the valuation effect of the month's currency movement within the same reporting month. Conditional volatility is constructed recursively from the daily returns of the same and preceding months. The two series thus share a single monthly shock under different timing conventions, and the Wald statistic loads the shared component on the profitability side. The weak reverse direction is consistent with this account, although insignificant coefficients cannot by themselves establish the absence of a structural channel from volatility to profitability. The reading is supported by the significantly negative quantile-on-quantile coefficients for profitability, which show that volatility depresses earnings even under calm conditions while the causality test attributes the shared monthly variation to the profitability side.

Three implications follow for policy. The first concerns measurement. Artificial accounting rules and prolonged forbearance improve published indicators in the short run while allowing the underlying position to deteriorate, and the closure of the early intervention window raises the eventual cost of resolution. Capital regulation on its own does not discipline bank risk, and its effect varies with the period and with bank characteristics [43,58]. Because a falling non-performing loan ratio and a rising capital ratio may both reflect denominator inflation during currency stress, supervisors require organic measures that strip revaluation and forbearance effects from the reported figures. Stress testing for Turkish bank credit risk under currency scenarios already exists in the literature [59-62], and extending such designs to quantify the gap between reported and organic ratios is feasible with supervisory data. Stronger supervisory capacity raises the cost of constructing artificial buffers [57], and inspection intensity directly affects the extent of concealment [32].

The second implication concerns timing. Since exposure is built while the currency is calm, preventive instruments must bind in exactly those periods. Dynamic provisioning accumulates reserves during phases that appear sound on paper, and binding limits on unhedged foreign currency lending remove the incentive at its source. Acharya and Vij [23] show that caps on foreign borrowing costs break the carry trade relationship. Ahnert *et al.*, [7] add the necessary caveat, since foreign exchange regulation applied to banks alone displaces exposure to direct corporate issuance and leaves aggregate vulnerability in place. Coverage of the perimeter therefore matters as much as the stringency of the rule. The third implication concerns instrument selection. Credit expansion carries substantial macroeconomic consequences in Türkiye, and the credit channel occupies a central place in policy transmission [58]. Macroprudential tools are effective during credit surges and sudden stops [59], they deter corporate leverage under uncertainty [60], and consumer credit regulation demonstrably alters borrowing behaviour [61]. What connects these three levels is a single requirement, namely that supervision be directed at the mechanisms generating the indicators rather than at the indicators themselves.

6. Conclusions

This study examined how exchange rate volatility affects the stability of the Turkish banking sector across the distributions of both variables and across time and frequency, and it found a relationship that no average effect can represent. Volatility raises the non-performing loan ratio during tranquil periods, with the effect strengthening markedly where the ratio is already high, while the same relationship turns negative under severe currency stress. Capital adequacy improves in reported terms when sector capital is weakest and deteriorates when it is strongest. Profitability is eroded even under calm conditions, and its apparent predictive power over volatility traces to valuation results embedded in monthly earnings rather than to any structural channel. The dominant direction runs from volatility to the sector, and the sign reversals survive changes in bandwidth, the addition of macroeconomic controls and an alternative volatility measure. What generates these reversals is denominator inflation together with supervisory discretion over classification windows and valuation dates, not any improvement in bank soundness. Indicators that move in a reassuring direction during currency stress may therefore conceal deterioration precisely when detection matters most. Two conclusions follow. Surveillance requires organic measures constructed net of revaluation and forbearance effects, since reported ratios respond to the regulatory calendar as much as to credit fundamentals. And because exposure accumulates while the currency is calm, macroprudential instruments must bind in those periods and reach borrowing outside the banking perimeter, since corrective action arrives only after the recognition window has closed.

Appendix A

Table A1 reports the complete set of quantile-on-quantile estimates obtained with the macroeconomic control set discussed in subsection 4.6.

Table A1

Partial quantile-on-quantile estimates with macroeconomic controls, December 2003 to December 2025, 265 observations

Dependent variable	θ	τ	β(θ,τ)	95 percent bootstrap CI
NPL	0.10	0.10	0.659	[−1.253, 1.615]
NPL	0.50	0.10	0.271	[−2.456, 4.572]
NPL	0.90	0.10	−0.282	[−0.744, 0.299]
NPL	0.10	0.50	0.120	[−1.726, 3.493]
NPL	0.50	0.50	1.634	[−5.374, 9.460]
NPL	0.90	0.50	0.180	[−0.652, 0.809]
NPL	0.10	0.90	2.157	[−0.944, 10.358]
NPL	0.50	0.90	6.686	[−4.098, 9.089]
NPL	0.90	0.90	1.096	[−0.562, 1.973]
CAR	0.10	0.10	−7.437	[−12.077, 1.623]
CAR	0.50	0.10	−8.126	[−19.065, 15.957]
CAR	0.90	0.10	−1.082	[−2.504, 0.778]
CAR	0.10	0.50	−4.395	[−9.293, 4.298]
CAR	0.50	0.50	8.921	[−10.090, 24.337]
CAR	0.90	0.50	−0.281	[−2.284, 0.917]
CAR	0.10	0.90	6.190	[−6.984, 20.988]
CAR	0.50	0.90	11.501	[−9.292, 35.779]

Table A1
Continued

Dependent variable	θ	τ	β(θ,τ)	95 percent bootstrap CI
CAR	0.90	0.90	0.817	[−1.678, 2.348]
ROA	0.10	0.10	−7.471**	[−12.173, −0.559]
ROA	0.50	0.10	−0.647	[−7.438, 3.698]
ROA	0.90	0.10	0.258	[−1.012, 0.794]
ROA	0.10	0.50	−2.151	[−6.964, 3.019]
ROA	0.50	0.50	−0.408	[−8.219, 3.900]
ROA	0.90	0.50	−0.182	[−1.031, 0.396]
ROA	0.10	0.90	−0.243	[−4.482, 6.825]
ROA	0.50	0.90	−4.627	[−10.786, 3.716]
ROA	0.90	0.90	−0.011	[−0.672, 0.851]

Note. The control set contains monthly inflation, annual industrial production growth, the policy rate, the VIX, the United States ten-year yield and credit growth. Confidence intervals are obtained from 500 bootstrap replications and the bandwidth is h = 0.05. ***, ** and * indicate that the 99, 95 and 90 percent bootstrap confidence intervals exclude zero.

Funding
This research received no external funding.

Data Availability Statement
The data supporting the reported results are drawn from publicly accessible sources. Banking sector aggregates are obtained from the Turkish Banking Sector Monthly Bulletin of the Banking Regulation and Supervision Agency. Exchange rate data are constructed from European Central Bank reference rates. The consumer price index and the industrial production index are obtained from OECD SDMX databases, the policy rate from the interest rate statistics of the Central Bank of the Republic of Türkiye, and the VIX index and the United States ten-year Treasury yield from the FRED database. The processed data set and the estimation code are available from the author on reasonable request.

Conflicts of Interest
The author declares that there is no known competing financial interest or personal relationship that could have appeared to influence the work reported in this paper.

Acknowledgement
This research was not funded by any grant.

References

[1] Barry, E., Rose, A. K., & Wyplosz, C. (1996). Contagious currency crises: First tests. *Scandinavian Journal of Economics*, 98(4), 463–484. https://doi.org/10.2307/3440879
[2] Gaies, B., Goutte, S., & Guesmi, K. (2019). Banking crises in developing countries–What crucial role of exchange rate stability and external liabilities? *Finance Research Letters*, 31, 436–447. https://doi.org/10.1016/j.frl.2018.12.014
[3] Akinci, Ö., & Queralto, A. (2024). Exchange rate dynamics and monetary spillovers with imperfect financial markets. *The Review of Financial Studies*, 37(2), 309–355. https://doi.org/10.1093/rfs/hhad078
[4] Abbassi, P., & Bräuning, F. (2023). Exchange rate risk, banks' currency mismatches, and credit supply. *Journal of International Economics*, 141, 103725. https://doi.org/10.1016/j.jinteco.2023.103725
[5] Kadırgan, C. (2023). Exchange rate driven balance sheet effect and capital flows to emerging market economies. *The Quarterly Review of Economics and Finance*, 87, 35–45. https://doi.org/10.1016/j.qref.2022.11.003

[6] Kuzucu, N., & Kuzucu, S. (2019). What drives non-performing loans? Evidence from emerging and advanced economies during pre-and post-global financial crisis. *Emerging Markets Finance and Trade*, 55(8), 1694–1708. https://doi.org/10.1080/1540496X.2018.1547877

[7] Ahnert, T., Forbes, K., Friedrich, C., & Reinhardt, D. (2021). Macroprudential FX regulations: Shifting the snowbanks of FX vulnerability? *Journal of Financial Economics*, 140(1), 145–174. https://doi.org/10.1016/j.jfineco.2020.10.005

[8] Fischer, A. M., & Yeşin, P. (2022). Foreign currency loan conversions and currency mismatches. *Journal of International Money and Finance*, 122, 102499. https://doi.org/10.1016/j.jimonfin.2021.102499

[9] Avdjiev, S., Bruno, V., Koch, C., & Shin, H. S. (2019). The dollar exchange rate as a global risk factor: Evidence from investment. *IMF Economic Review*, 67(1), 151–173. https://doi.org/10.1057/s41308-019-00074-4

[10] Bruno, V., & Shin, H. S. (2015). Capital flows and the risk-taking channel of monetary policy. *Journal of Monetary Economics*, 71, 119–132. https://doi.org/10.1016/j.jmoneco.2014.11.011

[11] Borio, C., & Zhu, H. (2012). Capital regulation, risk-taking and monetary policy: A missing link in the transmission mechanism? *Journal of Financial Stability*, 8(4), 236–251. https://doi.org/10.1016/j.jfs.2011.12.003

[12] Caglayan, M., Pham, T., & Talavera, O. (2021). Dollarization, pass-through, and domestic lending: Evidence from Turkish Banking. *Emerging Markets Finance and Trade*, 57(11), 3190–3201. https://doi.org/10.1080/1540496X.2019.1678146

[13] Demirkılıç, S. (2021). Balance sheet effects of foreign currency debt and real exchange rate on corporate investment: Evidence from Turkey. *Emerging Markets Review*, 47, 100796. https://doi.org/10.1016/j.ememar.2021.100796

[14] Kasman, S., Vardar, G., & Tunç, G. (2011). The impact of interest rate and exchange rate volatility on banks' stock returns and volatility: Evidence from Turkey. *Economic Modelling*, 28(3), 1328–1334. https://doi.org/10.1016/j.econmod.2011.01.015

[15] Ando, T., Greenwood-Nimmo, M., & Shin, Y. (2022). Quantile connectedness: Modeling tail behavior in the topology of financial networks. *Management Science*, 68(4), 2401–2431. https://doi.org/10.1287/mnsc.2021.3984

[16] Baumöhl, E., Bouri, E., Shahzad, S. J. H., & Výrost, T. (2022). Measuring systemic risk in the global banking sector: A cross-quantilogram network approach. *Economic Modelling*, 109, 105775. https://doi.org/10.1016/j.econmod.2022.105775

[17] Wang, J., Liu, T., & Pan, N. (2023). Analyzing quantile spillover effects among international financial markets. *The North American Journal of Economics and Finance*, 64, 101881. https://doi.org/10.1016/j.najef.2023.101881

[18] Yousaf, I., Youssef, M., & Goodell, J. W. (2022). Quantile connectedness between sentiment and financial markets: Evidence from the S&P 500 twitter sentiment index. *International Review of Financial Analysis*, 83, 102322. https://doi.org/10.1016/j.irfa.2022.102322

[19] Sim, N., & Zhou, H. (2015). Oil prices, US stock return, and the dependence between their quantiles. *Journal of Banking & Finance*, 55, 1–8. https://doi.org/10.1016/j.jbankfin.2015.01.013

[20] Umar, Z., Bossman, A., Choi, S. Y., & Teplova, T. (2022). Does geopolitical risk matter for global asset returns? Evidence from quantile-on-quantile regression. *Finance Research Letters*, 48, 102991. https://doi.org/10.1016/j.frl.2022.102991

[21] Bruno, V., & Shin, H. S. (2017). Global dollar credit and carry trades: A firm-level analysis. *The Review of Financial Studies*, 30(3), 703–749. https://doi.org/10.1093/rfs/hhw099

[22] Hardy, B., & Saffie, F. (2024). From carry trades to trade credit: Financial intermediation by non-financial corporations. *Journal of International Economics*, 152, 103988. https://doi.org/10.1016/j.jinteco.2024.103988

[23] Acharya, V. V., & Vij, S. (2025). Regulating carry trades: Evidence from foreign currency borrowing of corporations in India. *Review of Economic Studies*, 92(4), 2071–2107. https://doi.org/10.1093/restud/rdae089

[24] Kalemli-Ozcan, S., Liu, X., & Shim, I. (2021). Exchange rate fluctuations and firm leverage. *IMF Economic Review*, 69(1), 90–121. https://doi.org/10.1057/s41308-020-00130-4

[25] Niepmann, F., & Schmidt-Eisenlohr, T. (2022). Foreign currency loans and credit risk: Evidence from US banks. *Journal of International Economics*, 135, 103558. https://doi.org/10.1016/j.jinteco.2021.103558

[26] Ari, A., Chen, S., & Ratnovski, L. (2021). The dynamics of non-performing loans during banking crises: A new database with post-COVID-19 implications. *Journal of Banking & Finance*, 133, 106140. https://doi.org/10.1016/j.jbankfin.2021.106140

[27] Acharya, V. V., Borchert, L., Jager, M., & Steffen, S. (2021). Kicking the can down the road: Government interventions in the European banking sector. *The Review of Financial Studies*, 34(9), 4090–4131. https://doi.org/10.1093/rfs/hhab002

[28] Faria-e-Castro, M., Paul, P., & Sánchez, J. M. (2024). Evergreening. *Journal of Financial Economics*, 153, 103778. https://doi.org/10.1016/j.jfineco.2024.103778

[29] Tantri, P. (2021). Identifying ever-greening: Evidence using loan-level data. *Journal of Banking & Finance*, 122, 105997. https://doi.org/10.1016/j.jbankfin.2020.105997

[30] Blattner, L., Farinha, L., & Rebelo, F. (2023). When losses turn into loans: The cost of weak banks. *American Economic Review*, 113(6), 1600–1641. https://doi.org/10.1257/aer.20201623
[31] Kashyap, N., Mahapatro, S., & Tantri, P. (2023). Indirect evergreening using related parties: Evidence from India. *Journal of Financial and Quantitative Analysis*, 58(5), 2131–2161. https://doi.org/10.1017/S0022109022000412
[32] Bonfim, D., Cerqueiro, G., Degryse, H., & Ongena, S. (2023). On-site inspecting zombie lending. *Management Science*, 69(5), 2547–2567. https://doi.org/10.1287/mnsc.2022.4452
[33] Chopra, Y., Subramanian, K., & Tantri, P. L. (2021). Bank cleanups, capitalization, and lending: Evidence from India. *The Review of Financial Studies*, 34(9), 4132–4176. https://doi.org/10.1093/rfs/hhaa119
[34] Álvarez, L., García-Posada, M., & Mayordomo, S. (2023). Distressed firms, zombie firms and zombie lending: A taxonomy. *Journal of Banking & Finance*, 149, 106762. https://doi.org/10.1016/j.jbankfin.2023.106762
[35] Bassi, C., Behn, M., Grill, M., & Waibel, M. (2024). Window dressing of regulatory metrics: Evidence from repo markets. *Journal of Financial Intermediation*, 58, 101086. https://doi.org/10.1016/j.jfi.2024.101086
[36] Mariathasan, M., & Merrouche, O. (2014). The manipulation of basel risk-weights. *Journal of Financial Intermediation*, 23(3), 300–321. https://doi.org/10.1016/j.jfi.2014.04.004
[37] Behn, M., Haselmann, R., & Vig, V. (2022). The limits of model-based regulation. *The Journal of Finance*, 77(3), 1635–1684. https://doi.org/10.1111/jofi.13124
[38] Plosser, M. C., & Santos, J. A. (2018). Banks' incentives and inconsistent risk models. *The Review of Financial Studies*, 31(6), 2080–2112. https://doi.org/10.1093/rfs/hhy028
[39] Böhnke, V., Ongena, S., Paraschiv, F., & Reite, E. J. (2023). Back to the roots of internal credit risk models: Does risk explain why banks' risk-weighted asset levels converge over time? *Journal of Banking & Finance*, 156, 106992. https://doi.org/10.1016/j.jbankfin.2023.106992
[40] Ferri, G., & Pesic, V. (2017). Bank regulatory arbitrage via risk weighted assets dispersion. *Journal of Financial Stability*, 33, 331–345. https://doi.org/10.1016/j.jfs.2016.10.006
[41] Mayordomo, S., Rachedi, O., & Rodríguez Moreno, M. (2024). Bank regulatory capital arbitrage: Evidence from housing overappraisals. *Management Science*, 70(4), 2255–2271. https://doi.org/10.1287/mnsc.2023.4805
[42] Choi, D. B., Holcomb, M. R., & Morgan, D. P. (2020). Bank leverage limits and regulatory arbitrage: Old question–new evidence. *Journal of Money, Credit and Banking*, 52(S1), 241–266. https://doi.org/10.1111/jmcb.12742
[43] Anginer, D., Bertay, A. C., Cull, R., Demirgüç-Kunt, A., & Mare, D. S. (2024). Bank capital regulation and risk after the Global Financial Crisis. *Journal of Financial Stability*, 74, 100891. https://doi.org/10.1016/j.jfs.2021.100891
[44] Shaddady, A., & Moore, T. (2019). Investigation of the effects of financial regulation and supervision on bank stability: The application of CAMELS-DEA to quantile regressions. *Journal of International Financial Markets, Institutions and Money*, 58, 96–116. https://doi.org/10.1016/j.intfin.2018.09.006
[45] Jang, H., Kim, J. M., & Noh, H. (2024). Vine copula Granger causality in quantiles. *Applied Economics*, 56(10), 1109–1118. https://doi.org/10.1080/00036846.2023.2174941
[46] Qiao, X., Zhu, H., & Hau, L. (2020). Time-frequency co-movement of cryptocurrency return and volatility: Evidence from wavelet coherence analysis. *International Review of Financial Analysis*, 71, 101541. https://doi.org/10.1016/j.irfa.2020.101541
[47] Bollerslev, T. (1986). Generalized autoregressive conditional heteroskedasticity. *Journal of Econometrics*, 31(3), 307–327. https://doi.org/10.1016/0304-4076(86)90063-1
[48] Torrence, C., & Compo, G. P. (1998). A practical guide to wavelet analysis. *Bulletin of the American Meteorological Society*, 79(1), 61–78. https://doi.org/10.1175/1520-0477(1998)079%3C0061:APGTWA%3E2.0.CO;2
[49] Grinsted, A., Moore, J. C., & Jevrejeva, S. (2004). Application of the cross wavelet transform and wavelet coherence to geophysical time series. *Nonlinear Processes in Geophysics*, 11(5/6), 561–566. https://doi.org/10.5194/npg-11-561-2004
[50] Koenker, R., & Bassett Jr., G. (1978). Regression quantiles. *Econometrica*, 46(1), 33–50. https://doi.org/10.2307/1913643
[51] Chuang, C. C., Kuan, C. M., & Lin, H. Y. (2009). Causality in quantiles and dynamic stock return–volume relations. *Journal of Banking & Finance*, 33(7), 1351–1360. https://doi.org/10.1016/j.jbankfin.2009.02.013
[52] Dickey, D. A., & Fuller, W. A. (1979). Distribution of the estimators for autoregressive time series with a unit root. *Journal of the American Statistical Association*, 74(366a), 427–431. https://doi.org/10.1080/01621459.1979.10482531
[53] Phillips, P. C., & Perron, P. (1988). Testing for a unit root in time series regression. *Biometrika*, 75(2), 335–346. https://doi.org/10.1093/biomet/75.2.335
[54] Kwiatkowski, D., Phillips, P. C., Schmidt, P., & Shin, Y. (1992). Testing the null hypothesis of stationarity against the alternative of a unit root: How sure are we that economic time series have a unit root? *Journal of Econometrics*, 54(1-3), 159–178. https://doi.org/10.1016/0304-4076(92)90104-Y

[55] Zivot, E., & Andrews, D. W. K. (2002). Further evidence on the great crash, the oil-price shock, and the unit-root hypothesis. *Journal of Business & Economic Statistics*, 20(1), 25–44. https://doi.org/10.1198/073500102753410372
[56] Martynova, N., Perotti, E., & Suarez, J. (2022). Capital forbearance in the bank recovery and resolution game. *Journal of Financial Economics*, 146(3), 884–904. https://doi.org/10.1016/j.jfineco.2022.09.006
[57] Hirtle, B., Kovner, A., & Plosser, M. (2020). The impact of supervision on bank performance. *The Journal of Finance*, 75(5), 2765–2808. https://doi.org/10.1111/jofi.12964
[58] Büyükbaşaran, T., Karasoy-Can, G., & Küçük, H. (2022). Macroeconomic effects of bank lending in an emerging economy: Evidence from Turkey. *Economic Modelling*, 115, 105946. https://doi.org/10.1016/j.econmod.2022.105946
[59] Ekinci, M. F., Kenc, T., & Tamgac Tezcan, U. (2024). Effectiveness of macroprudential policies on credit surge and stop episodes. *Open Economies Review*, 35(5), 1085–1113. https://doi.org/10.1007/s11079-023-09744-3
[60] Yarba, I., & Güner, Z. N. (2020). Uncertainty, macroprudential policies and corporate leverage: Firm-level evidence. *Central Bank Review*, 20(2), 33–42. https://doi.org/10.1016/j.cbrev.2020.03.005
[61] Agarwal, S., Hadzic, M., Song, C., & Yildirim, Y. (2023). Liquidity constraints, consumption, and debt repayment: Evidence from macroprudential policy in Turkey. *The Review of Financial Studies*, 36(10), 3953–3998. https://doi.org/10.1093/rfs/hhad024
[62] Aydemir, R., Atik, Z., & Guloglu, B. (2024). Macro stress testing the credit risk of conventional and participation banks in Turkey: A nonparametric quantile regression approach. *Eastern European Economics*, 62(6), 727–761. https://doi.org/10.1080/00128775.2023.2253226